APPENDIX 3: ARCHAEOMETALLURGICAL RESIDUES FROM CINDER HILL, CUTACRE

Tim Young

A sizable assemblage of archaeometallurgical residues was recovered during the excavation at the late medieval bloomery site at Cinder Hill (Site 42N), Cutacre (*Ch 3, p 44*). This material was initially assessed (OA North 2010), then 16 samples were analysed. The aim of this was to determine more closely the main residues identified and, in turn, the metalworking process(es) that occurred at the site.

The total assemblage amounted to *c* 200 kg. Of this, 114 kg was unstratified, the remainder deriving from the fills of a variety of cut features, including pits, a gully, and at least two, and possibly as many as six, slag-tapping bloomery furnaces. The distribution of slag facies was established by context (Table 15).

The assemblage was dominated by tapped bloomery iron-smelting slags, with a total weight of 143 kg. These tapped slags were divisible, approximately equally, into dense varieties and those that were much more highly vesicular, giving them a low bulk density. Most of the tapped slags were in rather small fragments, so there is no certain evidence for the amount of slag produced by individual smelts. Although a plan of furnace ***722***/***720*** (*Ch 3, p 47*) shows an *in-situ* slag flow, this was not lifted.

Slags that cooled within the furnaces are more difficult to identify within the collection. The initial assessment of the assemblage (Young 2007) identified 2.5 kg of charcoal-rich slags that were probably furnace slags, 30.9 kg of plano-convex or biconvex slag cakes, interpreted as probably being smithing slags, together with 7.9 kg of other, indeterminate, curved slag crusts. Detailed investigation of representative material suggests that much of this material was from smelting, and originated as slag 'bowls' in the lower part of the furnace.

Some of the smithing-hearth cake-like material did indeed derive from smithing. One of the small plano-convex cakes is a smithing slag and possessed a vesicular, wustite-rich, microstructure. Wustite-rich slag was also found within a large (3.8 kg) cake, rich in metallic iron. The high loss of iron to the hearth, the low degree of incorporation of hearth lining, and the presence of large amounts of partially oxidised iron suggest that these slags were formed early in the process of bloom compaction, immediately after removal from the furnace.

There was also 11.7 kg of slag that was too fragmented for certain allocation to these classes of material. Furnace ceramic was represented by just 4.7 kg of fragments. The collections also included approximately 380 g of fragments of claystone ironstones.

Methodology

The materials were all examined visually (with a low-powered hand lens or microscope when required) as part of the assessment (*ibid*). An analytical programme entailing detailed investigation of a suite of residues, including slags, ores, and furnace ceramic, was developed to address the characterisation and interpretation of the origin of the assemblage. Sixteen samples (CUT1-CUT16; Table 16) were therefore selected for full chemical analyses, with five of those also selected for examination by scanning electron microscope (SEM).

The selected samples were slabbed on a diamond saw. Sub-samples were crushed for preparation of whole-sample chemical analyses and mounted for investigation in the scanning electron microscope in 25 mm-diameter blocks.

During the sample-selection process, a slag cake that had been identified during the assessment as a probable smithing slag proved to be an unusual metal-rich, bloom-like mass. This was slabbed, divided in two, and mounted as two 70 x 40 mm blocks (CUT17/18), of which one was then also examined as far as possible within the constraints of the project.

Chemical analysis was undertaken using two techniques. The major elements (Silicon (Si),

Context		Residue class:													Total slag (kg)
		dense tap	*vesicular tap*	*furnace bowl*	*charcoal-rich*	*brecciated*	*SHC*	*indeterminate crusts and bowls*	*indeterminate other*	*lining*	*ore*	*coal*	*concretion*	*iron object*	
500	topsoil	41.571	35.422	2.460	1.150	0.470	3.756	23.96	4.909	0.978	0.084	0.400	0.612	0.278	***114.685***
501	topsoil	0.664	0.456		0.128							0.016			***1.248***
503	possible hearth/ furnace	0.862	1.310						0.460		0.096	0.001			***2.632***
505	burnt layer	0.930	1.230					0.744	0.824						***3.728***
571	fill of pit ***572***	1.256						1.290	0.764						***3.310***
577	fill of possible furnace ***578***	7.484	21.489					1.680	1.650	0.458	0.106				***32.761***
584	fill of tapping pit ***581***	1.695	1.450					0.116	0.070						***3.331***
587	fill of tapping pit ***581***	1.015	2.575		0.790				0.200	0.244					***4.824***
589	fill of furnace ***588***	0.548			0.296			0.334	0.744	1.018					***2.940***
597	fill of pit ***596***	4.505	4.170	0.756	0.086			0.475	0.146	1.520	0.112	0.596		0.190	***11.658***
598	fill of ?pit ***599***	2.103	3.718					0.286				0.108	0.220	0.044	***6.107***
600	topsoil														***0.000***
701	fill of gully ***700***	3.650						0.626			0.050		0.020		***4.276***
704	fill of ?roothole ***705***	0.574	0.878						0.486						***1.938***
718	fill of possible pit ***719***	0.420					0.280	0.318	0.278				0.336		***1.296***
720	cut of tapping pit	0.168	1.180												***1.348***
723	fill of small furnace ***722***	0.284						0.224		0.502					***1.010***
733	fill of pit ***734***	0.422	0.660					1.396	0.960				1.145		***3.438***
739	fill of root disturbance ***738***	0.194						0.112	0.206						***0.512***
		68.345	***74.538***	***3.216***	***2.45***	***0.47***	***4.045***	***31.561***	***11.697***	***4.720***					***201.042***

Note: SHC = smithing-hearth cakes

Table 15: Summary of residue type by context

Sample	Context	Sample	Chemical analysis	SEM	Description
CUT1	***577***	1229	y		Small exfoliating weathered claystone nodule fragment with well-developed crust, *c* 4 mm thick and paler interior
CUT2	***577***	1238	y		Small, slightly exfoliating, claystone nodule
CUT3	***577***	1226	y		Rounded dense slag nub or flow lobe with a maximum thickness of 25 mm, 70 x 45 mm in plan. Top smooth with wrinkles suggestive of deflated lobes, base roughly microdimpled. Interior has extremely large olivine crystals
CUT4	***577***	1226	y		Flow lobe of very dense tap-slag with smooth maroon metallic surface, maximum 20 mm thick, base with dimples and tiny fuel moulds
CUT5	***587***	1244	y	y	Margin of a thin, very dense tap-slag flow, maximum thickness 15 mm
CUT6	***577***	1229	y		Highly vesicular tapped slag in sheet 40 mm thick. Top has irregular area near margin, both otherwise rather smooth with a few dimples. The base is strongly lobate with flows indicating the slab was inclined - *ie* it is the margin of a cake 90 mm thick and 100 mm laterally of inclined side to base (rest of profile not known, but deflated, with 60 mm concavity internal (*ie* on base it is just 30 mm thick)). Internally highly vesicular; large vesicles may actually be the centres of the original flow lobes?
CUT7	***587***	1244	y	y	Slice of tapped cake, 65 mm in centre, thinning over 110 mm to margin. Base roughly microdimpled, showing lobes very close to margin. Basal part is crust 8-10 mm in maximum thickness, overlain by vesicular slag, becoming tubular vesicular towards top. Line of large rounded vesicles at about centre height, but otherwise no internal stratification. Top strongly lobate, with some deflated lobes
CUT8	***597***	1222	y		Biconvex fragment, 130 mm wide, basal section, dense bladed, 30 mm thick, horizontal interface at top. Upper part 45 mm thick to zero on margin, highly vesicular, particularly towards base, with vesicles decreasing and fining upwards. Top rounded smooth, possibly slightly lobate, base roughly microdimpled
CUT9			y		(second upper sample from the above cake)
CUT10	***577***	1226	y		40 mm wide, 35 mm deep, frothy runner, with curved flow ridge on top and with smooth sides
CUT11	***587***	1244	y		A fragment of chaotic slag, with large voids, has several irregular faces with smooth and dimpled surfaces, but these do not indicate orientation. Internally vesicular with some fine charcoal inclusions
CUT12	***597***	1222	y		A large irregular block of indurated furnace lining, heavily slagged and altered, 85 mm thick
CUT13	***500***	1204	y	y	*c* 60% of biconvex cake (if regularly shaped). A very dense cake with columnar textures in lower part at least, with a smooth top with gently dimpled margins and a smooth base showing small-scale prills towards the margins. 200 mm wide, surviving length 130 mm, 67 mm maximum thickness
CUT14			y	y	(second upper sample from the above cake)
CUT15	***718***	1240	y		Rounded margin of a slag cake, with a flat top with broad dimples and somewhat wispy peaks between, and a base with fine dimples. The margin curves quickly so base and top parallel, 45-50 mm apart. Very dense, but with large irregular internal vesicles
CUT16	***500***	1204		y	160 x 150 x 90 mm block-like concavo-convex smithing-hearth cake, with slightly dished 'top' and slightly dimpled 'base'. Now sufficiently exploded to reveal iron core

SEM: Scanning Electron Microscope

Table 16: Samples selected for detailed analysis

Aluminium (Al), Iron (Fe), Manganese (Mn), Magnesium (Mg), Calcium (Ca), Sodium (Na), Potassium (K), Titanium (Ti), and Phosphorus (P); Table 17) were determined by X-Ray Fluorescence, using a fused bead on the Wavelength-Dispersive X-Ray Fluorescence (WD-XRF) system in the Department of Geology, Leicester University (this also generated analyses for Sulphur (S), Vanadium (V), Chromium (Cr), Strontium (Sr), Zirconium (Zr), Barium (Ba), Nickel (Ni), Copper (Cu), Zinc (Zn), Lead (Pb), and Hafnium (Hf); Table 18). Whole-specimen chemical analysis for 36 minor and trace elements (Scandium (Sc), Vanadium (V), Chromium (Cr), Cobalt (Co), Nickel (Ni), Copper (Cu), Zinc (Zn), Gallium (Ga), Rubidium (Rb), Strontium (Sr), Yttrium (Y), Zirconium (Zr), Niobium (Nb), Molybdenum (Mo), Tin (Sn), Caesium (Cs), Barium (Ba) (Table 19), Lauthanium (La), Cerium (Ce), Praseodymium (Pr), Neudymium (Nd), Samarium (Sm), Europium (Eu), Gadolinium (Gd), Terbium (Tb), Dysprosium (Dy), Holmium (Ho), Erbium (Er), Thulium (Tm), Ytterbium (Yb), Lutetium (Lu), Hafnium (Hf), Tantalum (Ta), Lead (Pb), Thorium (Th), and Uranium (U); Table 20) were undertaken using a sample in solution on the Thermo-Elemental X-series Inductively Coupled Plasma Mass Spectrometer (ICP-MS) in the School of Earth and Ocean Sciences, Cardiff University (this also generates lower-quality results for Iron (Fe), Manganese (Mn), Titanium (Ti), and Phosphorus (P) that are used mainly for quality-assurance purposes; Table 21).

Description of Residues

Tapped bloomery slags

The tapped bloomery slags showed a range of morphology from dense examples, with low vesicularity and a smooth, shiny, ropey surface (often with a slightly maroon tint), through to strongly vesicular varieties. The dense tapped slag occurred in small flows, often just a single layer of flow lobes in thickness, and usually less than 35 mm thick. There were no substantial accumulations, apart from material from fill ***701*** (of gully ***700***; *Ch 3, p 49*), which included a block with the steep side of an accumulation of dense flow lobes.

The vesicular slags included some with a morphology close to that of the dense tap slags, but most formed more massive blocks, some in rounded masses that appeared to have been less fluid than the typical textures of tapped slag. Some blocks provided evidence for vertical differentiation within the slag accumulation, with a moderately dense basal crust, overlain by extremely vesicular material, which in turn graded up into a slightly denser upper surface with or without flow lobes. This upper layer was seen to be cut by vertically aligned tubular vesicles in several specimens, suggesting degassing of the lower parts of the slag puddle. The differentiated textures occurred in blocks likely to have been from accumulations, 30-80 mm thick.

Where strongly flow-lobed textures (resembling those of the dense slags) were seen, they either seemed to be in thin flows or formed the margins of the more substantial puddles. The vesicular slags showed no evidence for accumulation as a stack of lobes, but appeared homogeneous, except where lobation had developed as a result of small rivulets of slag at the margins of the main mass. In the case of the largest blocks of vesicular slag, a possible origin within the furnace cannot be ruled out. The mineralogy and microstructure of two samples of certain tapped slag were examined in detail.

Sample CUT5: Furnace *588/581* (fill *587*)

The sample was from the margin of a dense, but locally highly vesicular, tapped-slag flow. The slag was finely vesicular, with some intergranular porosity in the interior of the lobes (Pl 177). The dominant microstructure comprised elongate olivine of up to 2 mm in length (Pl 178a; Pl 178b; Pl 178e), set in a groundmass containing extremely fine dendritic structures (probably also olivine) in glass. The main-phase olivine was relatively homogeneous, being a fayalite (iron silicate) with 1.2-1.4% forsterite (magnesium silicate; Fo), and overall levels of calcium substitution of 0.15-0.24% and 3.7-3.9% of manganese substitution (Fig 129). The margins of the lobes were formed by a crust 3-5 μm thick. These have a composition suggestive of haematite externally, but the inner parts show elevated manganese and may be of magnetite (both oxides of iron). The inner face of the crust is abrupt and planar, forming the substrate for the nucleation of small angular dendrites extending up to approximately 40 μm into the interior (Pl 178c). Single-crystal analyses were not possible on these tiny minerals, but mixed analyses suggested that they may have included hercynitic spinels.

The internal join of two lobes did not show an oxide rim (Pl 178e; Pl 178f), indicating these margins were not exposed to the air. Close to this point, where the external margin again appears (Pl 178f; Pl 178g), fine-scale alteration of the olivine into (presumably) iron oxides and a silica polymorph may be observed just below the lobe surface. This secondary decomposition of the olivine is unusual, but has been observed in situations where hot slag has interacted with volatiles, particularly steam (*eg* Young 2014b, fig 13).

	Class	SiO_2	Al_2O_3	Fe_2O_3	FeO	MnO	MgO	CaO	Na_2O	K_2O	TiO_2	P_2O_5	LOI	Total
CUT1	Ore	3.00	1.80	80.93	72.84	0.50	0.09	<0.003	<0.010	0.06	0.06	0.112	13.16	***99.82***
CUT2	Ore	5.86	2.81	73.10	65.79	0.69	0.36	0.24	0.02	0.51	0.16	0.326	15.18	***99.39***
CUT3	Dense nub	37.07	13.05	40.47	36.42	3.90	0.60	1.37	0.30	1.19	0.38	0.355	-4.19	***99.50***
CUT4	Dense tap slag	29.11	6.06	59.80	53.82	2.29	0.19	0.26	0.25	0.80	0.30	0.377	-5.49	***100.08***
CUT5	Dense tap slag	30.85	8.10	56.45	50.80	1.88	0.20	0.43	0.22	0.77	0.30	0.375	-2.87	***100.18***
CUT6	Vesicular tap slag	33.10	6.72	54.36	48.92	3.15	0.21	0.26	0.31	0.79	0.34	0.359	-4.71	***100.38***
CUT7	Tapped cake	33.03	6.11	52.34	47.11	4.88	0.18	0.16	0.30	0.75	0.32	0.372	-5.15	***99.57***
CUT8	Biconvex cake #1	29.61	5.79	59.72	53.75	2.00	0.18	0.24	0.23	0.63	0.26	0.685	-5.83	***99.86***
CUT9	Biconvex cake #1	30.23	6.03	58.64	52.77	2.07	0.17	0.27	0.25	0.67	0.28	0.713	-5.17	***99.86***
CUT10	Runner	29.36	8.97	48.45	43.61	7.12	0.51	1.13	0.21	0.83	0.31	0.661	-4.33	***99.24***
CUT11	Chaotic slag	38.83	7.73	44.58	40.12	2.43	0.20	0.42	0.33	0.86	0.34	0.386	3.61	***100.31***
CUT12	Lining	74.66	12.09	8.36	7.53	0.26	0.81	0.03	0.60	2.09	0.70	0.137	0.55	***100.61***
CUT13	Biconvex cake #2	23.70	5.98	67.28	60.55	0.93	0.22	0.50	0.11	0.42	0.21	0.562	-4.43	***100.34***
CUT14	Biconvex cake #2	23.63	6.28	66.12	59.51	0.92	0.22	0.64	0.16	0.56	0.22	0.568	-5.11	***99.70***
CUT15	Smithing-hearth cake?	4.64	0.88	92.95	83.65	0.35	0.02	0.02	<0.010	0.04	0.09	0.706	-7.51	***99.78***

Note: The shaded column is an alternative expression of iron as Fe^2 oxide. < indicates where the element was below the detection limit (3σ). Where the loss-on-ignition (LOI) is positive, the sample composition has been recalculated to incorporate the LOI. SiO_2 = Silica Dioxide, Al_2O_3 = Alumina, Fe_2O_3 = Haematite, FeO = Iron Oxide, MnO = Manganese Oxide, MgO = Magnesium Oxide, CaO = Calcium Oxide, Na_2O = Sodium Oxide, K_2O = Potassium Oxide, TiO_2 = Titanium Oxide, P_2O_5 = Phosporus Pentoxide, LOI = Loss on Ignition

Table 17: Major elements determined by XRF, expressed as wt% oxides

	Class	SO_3	V_2O_5	Cr_2O_3	SrO	ZrO_2	BaO	NiO	CuO	ZnO	PbO	HfO_2
CUT1	Ore	0.018	0.005	<0.004	0.007	0.012	<0.006	<0.004	<0.003	0.018	0.016	<0.005
CUT2	Ore	0.023	<0.003	<0.004	0.012	0.018	<0.006	<0.004	<0.003	0.011	0.014	0.008
CUT3	Dense nub	0.184	0.031	0.008	0.006	0.040	0.223	<0.004	<0.002	0.014	0.017	<0.004
CUT4	Dense tap slag	0.120	0.011	0.007	0.003	0.038	0.247	<0.004	<0.002	0.017	0.016	<0.004
CUT5	Dense tap slag	0.246	0.018	0.010	0.008	0.033	0.130	<0.004	<0.002	0.014	0.017	0.007
CUT6	Vesicular tap slag	0.138	0.011	<0.004	0.009	0.038	0.310	<0.004	<0.002	0.017	0.016	0.007
CUT7	Tapped cake	0.109	0.014	0.004	0.006	0.040	0.558	<0.004	<0.002	0.017	0.016	0.009
CUT8	Biconvex cake #1	0.146	0.011	0.007	0.003	0.033	0.122	<0.004	<0.002	0.020	0.016	0.005
CUT9	Biconvex cake #1	0.161	0.011	0.007	0.008	0.033	0.135	<0.004	<0.002	0.020	0.016	0.010
CUT10	Runner	0.203	0.022	0.007	0.008	0.035	0.824	<0.004	<0.002	0.017	0.015	0.007
CUT11	Chaotic slag	0.113	0.014	0.005	0.003	0.037	0.198	<0.004	<0.002	0.024	0.014	0.009
CUT12	Lining	0.009	0.012	0.008	0.009	0.056	0.030	<0.004	<0.002	0.158	0.015	<0.003
CUT13	Biconvex cake #2	0.208	0.015	<0.004	0.011	0.026	0.065	<0.004	<0.002	0.013	0.017	<0.005
CUT14	Biconvex cake #2	0.156	0.018	<0.004	0.009	0.031	0.070	<0.004	<0.002	0.012	0.018	<0.005
CUT15	Smithing-hearth cake?	<0.003	<0.003	<0.004	0.009	0.018	<0.006	<0.004	<0.003	0.012	0.017	0.008

Note: < indicates where the element was below the detection limit (3σ). Where the loss-on-ignition is positive, the sample composition has been recalculated to incorporate this
SO_3 = Sulphur Trioxide, V_2O_5 = Vanadium Pentoxide, Cr_2O_3 = Chromium Oxide, SrO = Strontium Oxide, ZrO_2 = Zirconium Dioxide, BaO = Barium Oxide, NiO = Nickel Oxide, CuO = Copper Oxide, ZnO = Zinc Oxide, PbO = Lead Oxide, HfO_2 = Hafnium Dioxide

Table 18: Minor elements determined by XRF, expressed as wt% oxides

	Class	Sc	V	Cr	Co	Ni	Cu	Zn	Ga	Rb	Sr	Y	Zr	Nb	Mo	Sn	Cs	Ba
CUT1	Ore	15.3	50.6	14.4	30.6	9.0	14.9	65.7	2.2	3.4	12.7	63.4	59.7	0.82	0.63	2.64	0.17	98.12
CUT2	Ore	5.3	34.5	17.7	14.5	14.3	13.5	32.0	4.3	21.8	67.9	17.0	95.2	3.10	0.42	4.18	1.34	216.68
CUT3	Dense nub	14.2	185.4	88.5	67.9	1.5	13.9	31.7	6.1	53.2	116.6	38.0	231.7	6.91	0.91	2.36	2.28	2169.12
CUT4	Dense tap slag	6.8	91.1	349.1	46.3	133.3	6.5	40.2	6.6	40.8	60.8	16.4	198.1	4.49	0.72	0.43	1.71	2321.88
CUT5	Dense tap slag	7.9	114.8	62.8	39.9	33.6	9.8	30.0	4.9	40.2	68.2	17.9	214.7	5.86	0.55	0.16	1.47	1293.00
CUT6	Vesicular tap slag	7.2	99.6	71.8	52.0	33.9	15.9	65.5	7.4	43.0	66.3	18.2	240.8	6.44	0.86	0.37	2.04	2818.61
CUT7	Tapped cake	6.8	107.6	57.7	53.6	11.2	6.7	53.1	7.7	44.0	61.7	17.5	227.6	6.02	0.99	2.41	1.95	4997.76
CUT8	Biconvex cake #1	6.3	91.6	51.9	65.2	10.9	9.4	78.1	7.3	35.9	51.3	13.0	200.9	5.09	0.86	1.27	1.42	1309.19
CUT9	Biconvex cake #1	6.0	93.5	68.9	69.3	16.9	6.1	76.2	7.7	37.2	53.8	13.1	180.9	4.67	0.98	2.30	1.56	1412.38
CUT10	Runner	11.0	131.9	63.4	118.8	5.9	10.1	51.1	8.7	36.8	101.6	30.2	210.3	5.87	1.24	10.83	1.61	7479.87
CUT11	Chaotic slag	7.0	103.0	81.6	66.0	34.8	5.0	96.3	6.5	45.2	67.9	17.4	262.2	6.32	0.82	4.67	2.09	1950.18
CUT12	Lining	10.9	88.7	78.8	59.3	20.0	15.5	889.2	18.1	93.6	91.8	27.4	351.9	11.20	0.85	4.89	5.95	487.73
CUT13	Biconvex cake #2	6.4	124.6	45.2	24.3	4.5	12.2	10.1	4.5	16.6	48.6	10.4	138.6	3.37	0.64	3.87	0.57	759.71
CUT14	Biconvex cake #2	4.9	120.3	43.6	41.6	6.5	11.7	17.3	4.7	22.9	62.6	12.2	178.6	5.18	0.75	4.44	0.74	891.89
CUT15	Smithing-hearth cake?	1.9	26.6	12.2	35.2	6.4	10.2	6.0	5.3	2.7	22.2	3.1	80.8	1.61	3.23	4.49	0.10	291.90

Note: All values in parts per million. Sc = Scandium, V = Vanadium, Cr = Chromium, Co = Cobalt, Ni = Nickel, Cu = Copper, Zn = Zinc, Ga = Galluim, Rb = Rubidium, Sr = Strontium, Y = Yttrium, Zr = Zirconium, Nb = Niobium, Mo = Molybdenum, Sn = Tin, Cs = Caesium, Ba = Barium

Table 19: Trace and minor elements (group 1) by ICP-MS

	Class	La	Ce	Pr	Nd	Sm	Eu	Gd	Tb	Dy	Ho	Er	Tm	Yb	Lu	Hf	Ta	Pb	Th	U
CUT1	Ore	14.02	23.42	3.17	17.00	5.70	1.65	8.43	1.34	7.47	1.52	3.98	0.59	3.46	0.48	1.57	0.10	4.80	1.01	0.54
CUT2	Ore	11.31	23.80	2.78	11.74	2.83	0.70	2.97	0.40	2.36	0.41	1.06	0.16	0.97	0.14	2.33	0.24	7.26	2.11	0.65
CUT3	Dense nub	28.73	87.93	8.83	36.28	9.08	2.39	9.14	1.36	7.62	1.26	3.13	0.47	2.99	0.44	6.60	1.81	3.24	12.71	4.62
CUT4	Dense tap slag	16.24	41.57	4.50	18.13	4.20	1.15	3.90	0.56	3.29	0.56	1.55	0.26	1.64	0.23	5.54	0.90	2.50	5.97	2.25
CUT5	Dense tap slag	16.08	43.34	4.65	19.20	4.70	1.20	4.20	0.63	3.61	0.60	1.61	0.25	1.65	0.23	5.54	0.85	2.77	6.77	2.63
CUT6	Vesicular tap slag	17.03	46.68	4.64	18.77	4.20	1.28	3.93	0.59	3.37	0.60	1.64	0.24	1.70	0.27	6.43	1.13	3.42	6.17	2.16
CUT7	Tapped cake	17.49	48.81	4.82	19.18	4.38	1.49	4.21	0.60	3.46	0.61	1.65	0.25	1.71	0.26	6.19	1.34	3.33	6.03	2.16
CUT8	Biconvex cake #1	13.22	36.22	3.55	14.08	3.28	0.86	2.93	0.44	2.53	0.44	1.22	0.19	1.23	0.18	5.01	1.05	3.89	5.33	2.24
CUT9	Biconvex cake #1	13.74	38.09	3.63	14.47	3.30	0.87	3.16	0.46	2.61	0.46	1.24	0.20	1.25	0.19	5.03	1.22	3.56	5.53	2.30
CUT10	Runner	22.02	65.22	6.26	26.78	6.92	2.25	6.92	1.05	5.40	0.95	2.39	0.37	2.23	0.34	5.90	1.53	6.01	9.92	3.36
CUT11	Chaotic slag	18.90	51.17	4.77	19.61	4.68	1.13	4.22	0.65	3.45	0.61	1.66	0.28	1.67	0.25	7.60	1.60	8.58	8.03	3.14
CUT12	Lining	31.60	64.01	6.98	26.58	5.29	0.97	4.41	0.71	4.03	0.79	2.30	0.39	2.47	0.42	9.41	1.50	15.50	10.40	3.01
CUT13	Biconvex cake #2	9.91	24.39	2.57	11.04	2.79	0.66	2.55	0.38	2.06	0.36	0.98	0.16	0.99	0.14	4.15	0.58	2.43	6.70	1.28
CUT14	Biconvex cake #2	12.79	31.90	3.41	14.25	3.58	0.84	3.31	0.50	2.59	0.45	1.15	0.16	0.97	0.15	4.91	0.90	3.51	7.26	1.46
CUT15	Smithing-hearth cake?	3.60	7.46	0.75	3.28	0.77	0.19	0.63	0.10	0.59	0.12	0.30	0.05	0.33	0.05	2.47	0.29	2.32	1.10	0.49

Note: All values in parts per million. La = Lauthanium, Ce = Cerium, Pr = Praseodymium, Nd = Neudymium, Sm = Samarium, Eu = Europium, Gd = Gadolinium, Tb = Terbium, Dy = Dysprosium, Ho = Holmium, Er = Erbium, Tm = Thulium, Yb = Ytterbium, Lu = Lutetium, Hf = Hafnium, Ta = Tantalum, Pb = Lead, Th = Thorium, U = Uranium

Table 20: Trace and minor elements (group 2) by ICP-MS

	class	SiO_2	MnO	FeO	TiO_2	P_2O_5
CUT1	Ore	10.28	1.44	83.47	0.02	0.10
CUT2	Ore	15.30	1.32	78.46	0.14	0.31
CUT3	Dense nub	33.60	0.75	44.96	0.38	0.34
CUT4	Dense tap slag	21.61	1.12	66.30	0.29	0.35
CUT5	Dense tap slag	23.46	1.02	61.99	0.29	0.36
CUT6	Vesicular tap slag	27.26	1.00	60.48	0.33	0.34
CUT7	Tapped cake	30.22	0.95	56.92	0.31	0.36
CUT8	Biconvex cake #1	21.91	1.13	67.20	0.24	0.63
CUT9	Biconvex cake #1	22.93	1.09	64.19	0.25	0.66
CUT10	Runner	27.79	0.91	55.17	0.30	0.62
CUT11	Chaotic slag	40.87	0.75	46.60	0.35	0.32
CUT12	Lining	69.02	0.15	9.84	0.72	0.13
CUT13	Biconvex cake #2	15.25	1.27	72.65	0.16	0.48
CUT14	Biconvex cake #2	17.28	1.22	70.88	0.18	0.51
CUT15	Smithing-hearth cake?	2.77	1.73	91.88	0.05	0.65

Note: SiO_2 = Silica Dioxide, MnO = Manganese Oxide, FeO = Iron Oxide, TiO_2 = Titanium Oxide, P_2O_5 = Phosphorus Pentoxide

Table 21: Major elements determined by ICP-MS, expressed as wt% oxides

Sample CUT7: Furnace *588/581* (fill *587*)
The sample was taken from a tapped slag mass, 65 mm thick in the centre. The base was roughly microdimpled, with lobes visible close to the margin. The lower part of the section is a basal crust, 8-10 mm in maximum thickness, that is overlain by vesicular slag, becoming tubular vesicular towards the top. There was a zone of large rounded vesicles at about mid-thickness, but otherwise there was no internal stratification. The top was strongly lobate, with some deflated lobes.

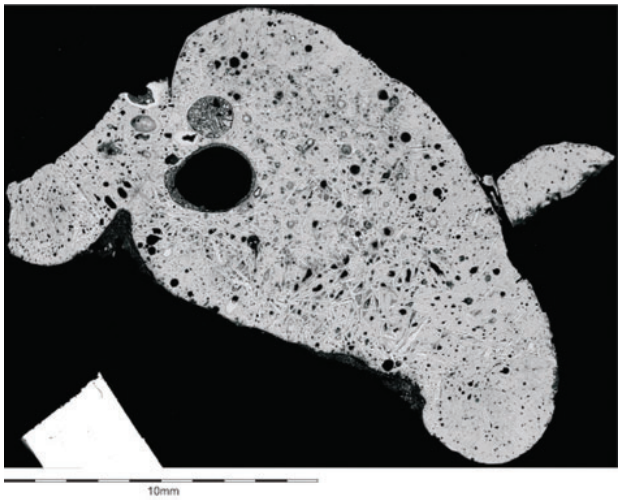

Plate 177: Backscattered electron image - CUT5, whole sample

The highly vesicular microstructure (Pl 179) comprised complex quenched olivine in broad crystals up to 2.5 mm in length, often with the appearance of having been disrupted into smaller blocky units (Pl 180a; Pl 180b). Between the main generation of olivine crystals were bundles (sheaves) of further olivine in geometric arrangements. The main olivine was fayalite with 1.4% (core) to 0.5% (margin) forsterite (Fo), and with overall levels of substitution by manganese of approximately 9.9%. Calcium was not detectable in most of the olivine (Fig 128).

Other samples
Chemical analysis was made of a further five examples of tapped slags and related materials (Table 16). Of these, two were not simple tapped slags: sample CUT11 was a slag in which iron-rich zones were mixed with entrained material dominated by melted lining, and also with abundant charcoal; sample CUT3 was a dense nub of partially devitrified dark glass, probably (given the unusual chemical composition) suggesting incorporation of an unusually ankeritic (calcium, magnesium, manganese carbonate) component of the ore charge.

Of the remaining samples, sample CUT4 was from a thin, dense, lobate slag sheet. The lobes

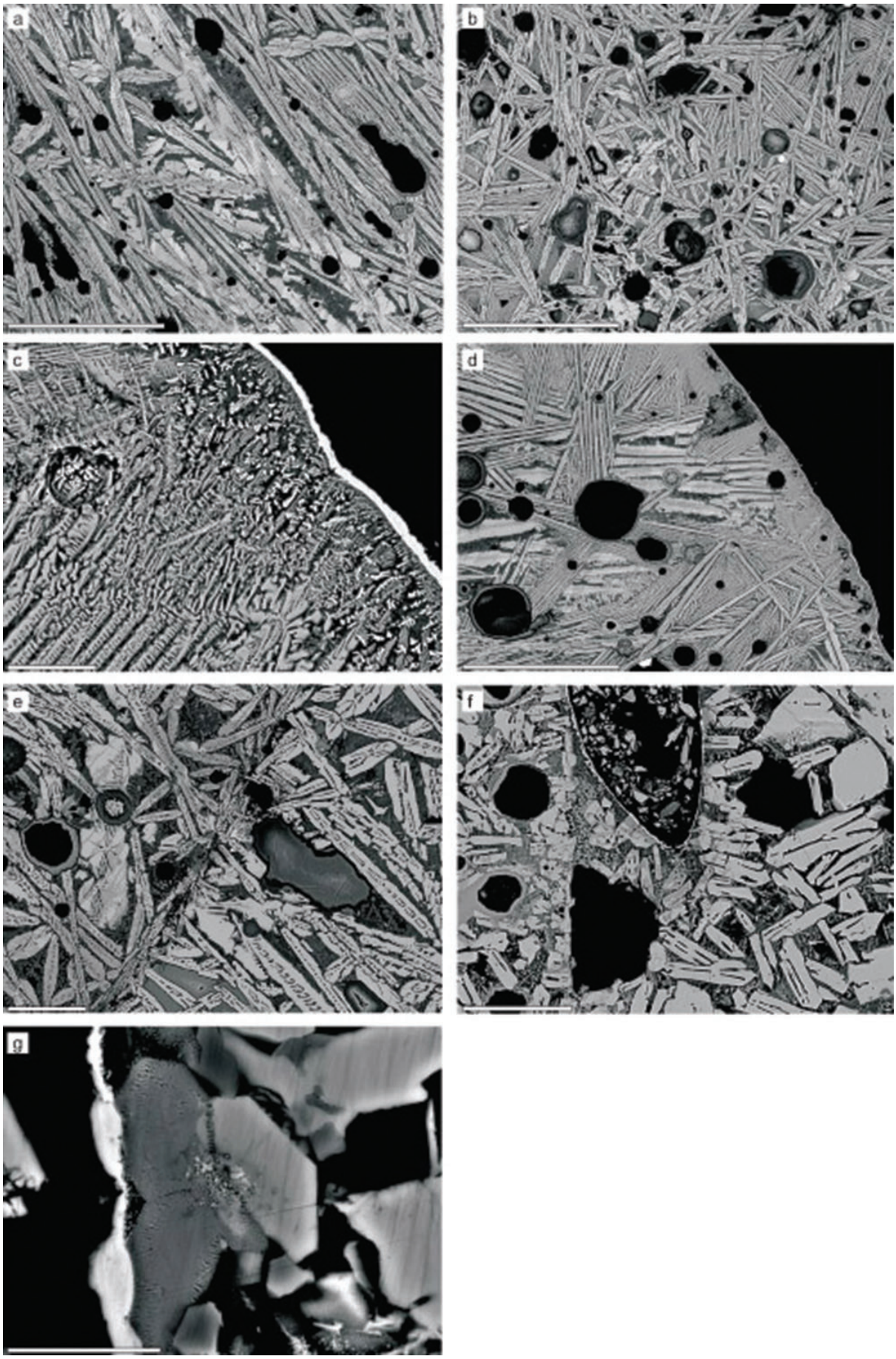

Plate 178: Backscattered electron images - CUT5

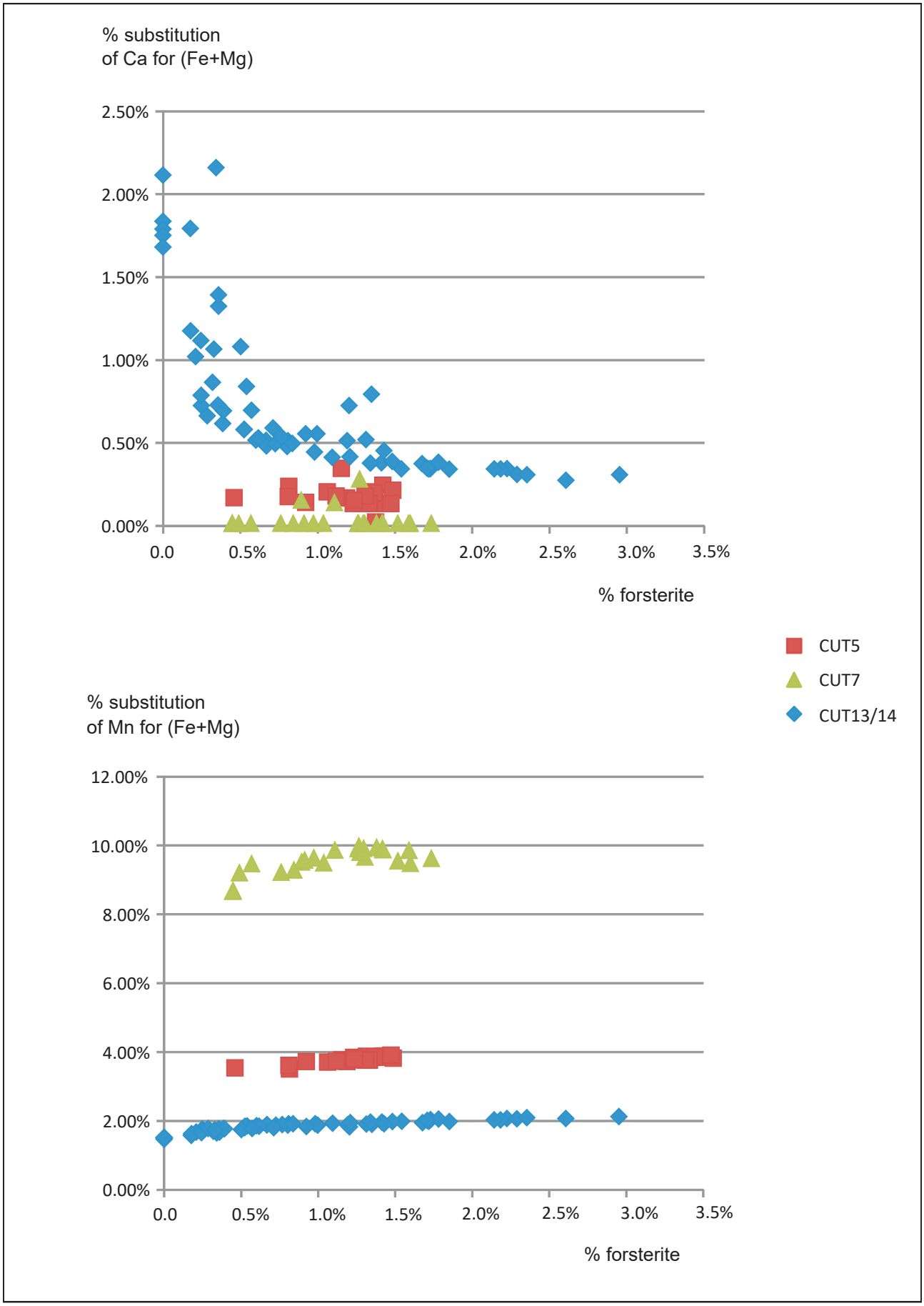

Figure 129: Variation in composition of the olivine present in the analysed samples

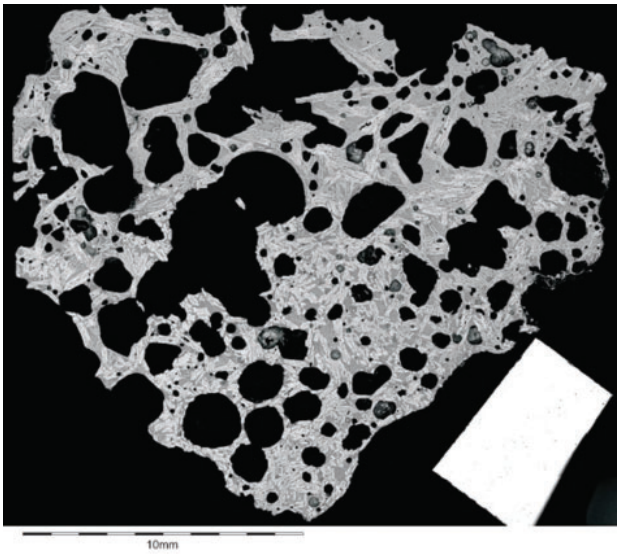

Plate 179: Backscattered electron image - CUT7, whole sample

were finely vesicular with long-bladed olivine. Sample CUT6 was a highly vesicular to 'frothy' tapped slag, with a highly lobed external (basal surface), but an upper surface dipping down into the tapped mass almost parallel to the base. This suggests deflation of the tapped slag cake, either because of onward movement of the slag through the tapping channel, or probably more likely, as a result of a very high degree of degassing of the frothy slag.

Sample CUT10 was taken from a short length of highly vesicular runner. There was a slight difference in the texture of one surface, suggesting it had formed as an open runner, rather than as a slag tube, as is common on some sites (*cf* Young 2014a). The slag was highly vesicular, but where broken horizontally, showed evidence for curved films between compressed vesicles, suggesting deformation under its final viscous flow.

Furnace slags

Various slag textures may be indicative of slags which cooled inside the furnace, including large vesicular blocks, a variety of slags with evidence for a high content of metallic iron (now highly weathered), slags with a high proportion of included charcoal debris (or charcoal moulds), and slag cakes resembling smithing-hearth cakes.

These slag textures are not entirely diagnostic; many are similar to textures seen in smithing slags. Those most similar to smithing-hearth cakes were mainly found within the material from the topsoil (***500***). They possessed basal crusts up to 35 mm in thickness, forming a bowl shape, which may either have a flat top or, if concave, contained an infill of more charcoal-rich or vesicular textures. The crusts may

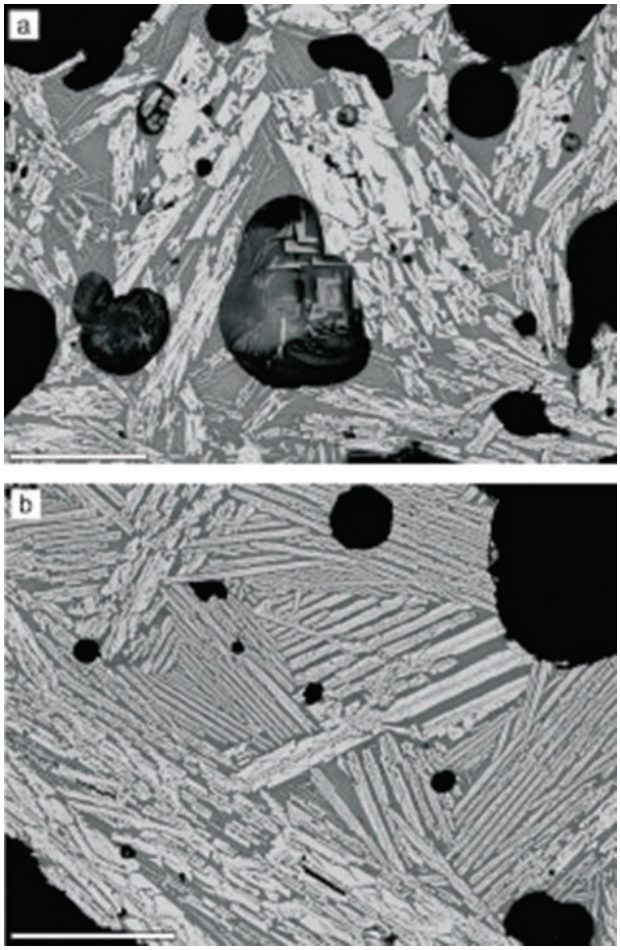

Plate 180: Backscattered electron images - CUT7

possess bladed olivine crystals, which in some cases were observed to have a crystal length equivalent to the entire thickness of the crust (30 mm). Two large biconvex blocks were selected for microstructural investigation on the SEM.

Sample CUT13/14: Topsoil (*500*)

Two samples were taken from a biconvex slag cake. If the cake was originally symmetrical, then approximately 60% survives, with a vertical fracture. The surviving part weighs 2460 g, suggesting an original weight of approximately 4100 g if the cake was symmetrical. It is 200 mm wide, with a surviving length of 130 mm, and a maximum thickness of 67 mm. The cake has a smooth convex top with gently dimpled margins, and a smooth base showing small-scale prills towards its edges.

The cake has a lower dense section with tubular vesicles (up to 30 mm thick), overlain by a thin dense zone with very little vesicularity, a zone with abundant fine sub-spherical vesicles, and then an intermittent zone of slag with low vesicularity, that is separated from the upper vesicular crust by a series of partially collapsed large voids (Pl 181).

Plate 181: Cut section through the biconvex slag block sampled as CUT13/14

The slag cake thus has some larger-scale features in common with the vesicular tapped-slag flows.

The microstructure in the lower vesicular part (sample CUT13; Pl 182) commences with rare isolated euhedral hercynite phenocrysts (large crystals) of up 100 μm (Pl 183a; Pl 183c). These have a composition equivalent to hercynite, with 11-14% magnetite, with cores reaching up to 0.006 atoms per formula unit (APFU) magnesium, 0.014 APFU titanium, 0.005 APFU vanadium, 0.003 APFU chromium, and 0.012 APFU manganese, and with less substituted margins.

The main mineral phase comprises stout complex olivine (up to 2 mm in length) in somewhat random orientations, with abundant spherical vesicles (up to 4.5 mm in diameter). Many of the vesicles show infill by later generations of finer olivine-rich slag (Pl 183b; Pl 183g). This main olivine typically shows a central zone in which the olivine is in a cotectic relationship with wustite (iron oxide, which forms dendritic growths spaced along a central wustite axis) and an outer zone with a cotectic relationship with hercynite (Pl 183d; Pl 183f). In some areas, an early olivine has no cotectic phases and is not structurally related to the orientation of the subsequent complex olivine.

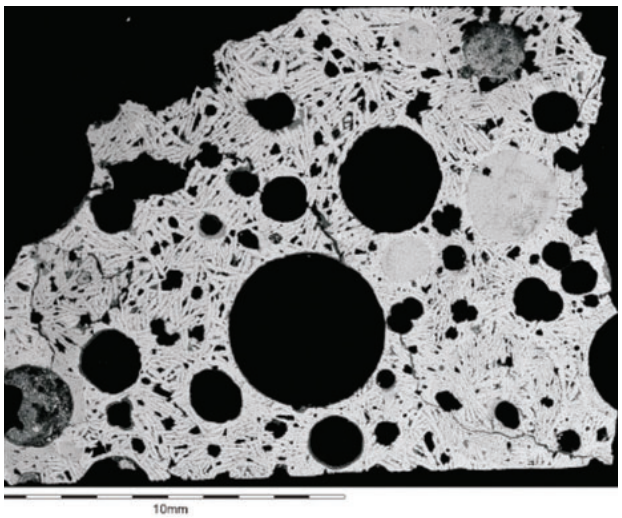

Plate 182: Backscattered electron image - CUT13, whole sample

The sample contains a single small (1.8 mm) rounded grain with a somewhat angular cellular texture (approximately 100 μm wide) of iron oxides, with a poorly defined, possibly glassy matrix, with a few large rounded and crescentic zones of aluminous glass (Pl 183a). This particle is interpreted as an incompletely reacted ore grain, with the cellular iron oxides suggestive of a relict texture after the original siderite (iron carbonate). The margin of the ore grain carries numerous examples of the early euhedral hercynite.

The sample from a coarsely vesicular upper section of the cake (sample CUT14; Pl 184) shows a crudely layered bulk structure, with varying degrees of vesicularity. The vesicles have been locally occluded by later generations of slag (Pl 185c), leading to a texture with even more contrasting grain sizes than in the lower part of the cake (*above*). The microstructures are similar in general to those of the lower part.

The compositions of the olivine in the two sections of this specimen show similar variation. For sample CUT14 from the upper part of the cake, the early simple olivine shows compositions from as high as (forsterite) Fo3, with 2.1% manganese substitution and 0.3% calcium substitution (Fig 128), down to Fo0.3, with 1.74% manganese substitution and 1.07% calcium substitution, whereas in sample CUT13, they do not extend to more than Fo1.3.

For the other contexts of olivine, the compositional ranges are more similar: for those in a cotectic with wustite, the range is from Fo1.8/2.2 down to Fo0.8/1.9, for those with hercynite, the main range is Fo1.5 (with 2.0% manganese and 0.34% calcium substitution) to Fo0.2 (with 1.73% manganese and 0.73% calcium substitution) and for the external margins, the composition ranges down to end-member fayalite, with 1.5% manganese and 2.2% calcium substitution. The overall compositional range of olivine in sample CUT13/14 is thus much greater than it is in the tapped-slag samples, CUT5 (Fo0.5 to Fo1.5) and CUT7 (Fo0.4 to Fo1.7).

The block from which samples CUT8/9 were taken was a fragment of a biconvex block approximately 70 mm thick. The lower 30 mm of the block comprises a dense, approximately plano-convex crust, with tubular vesicles and very large-bladed olivine crystals, above an irregular rough base. This zone is overlain by a highly vesicular slag, with large rounded vesicles of up to 30 mm, with the largest vesicles in the core of the block. The upper 20 mm of the block shows finer, but still abundant, vesicularity. The upper surface has raised wispy lobes, but no clear indication of flow.

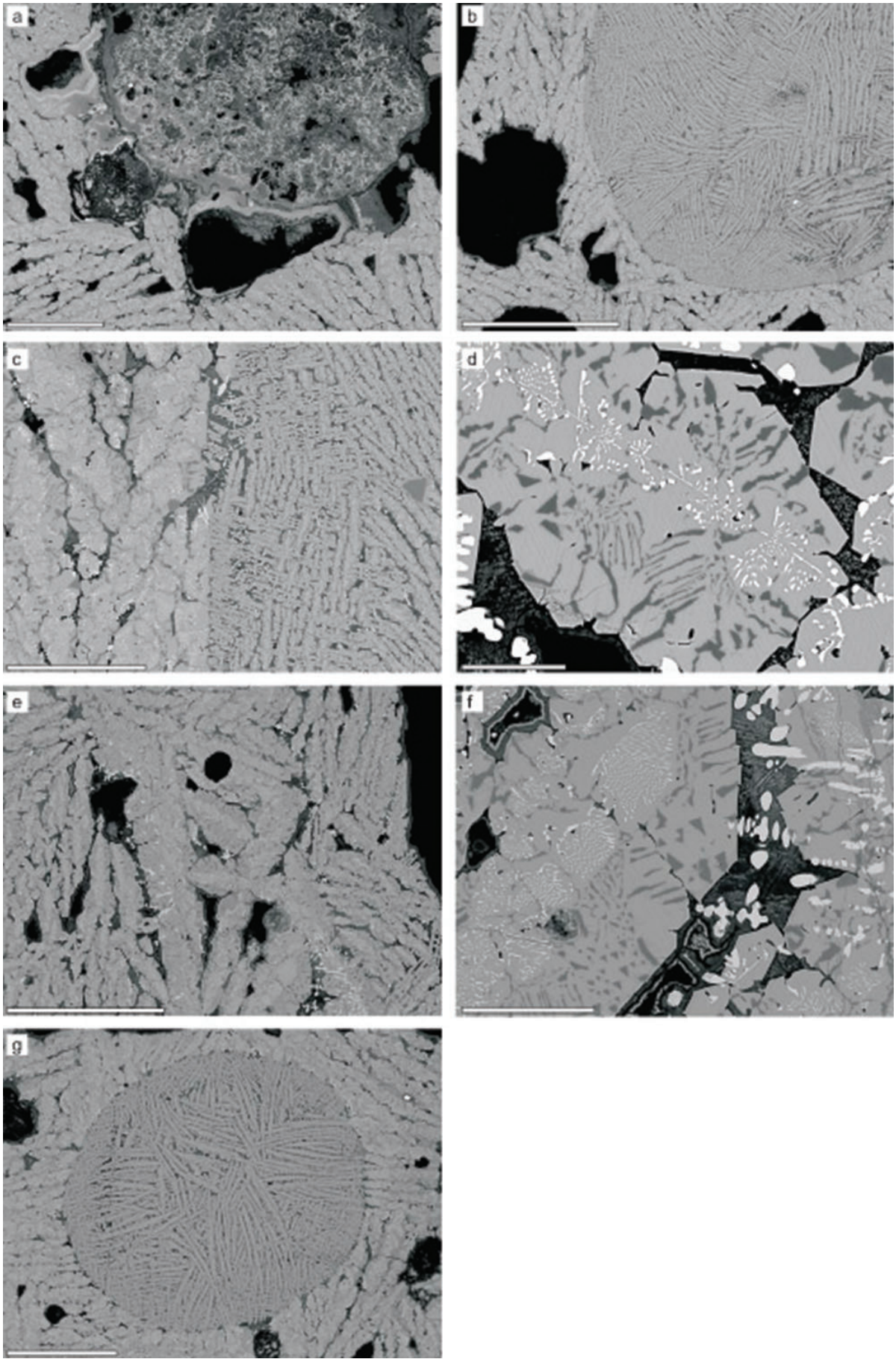

Plate 183: Backscattered electron images - CUT13

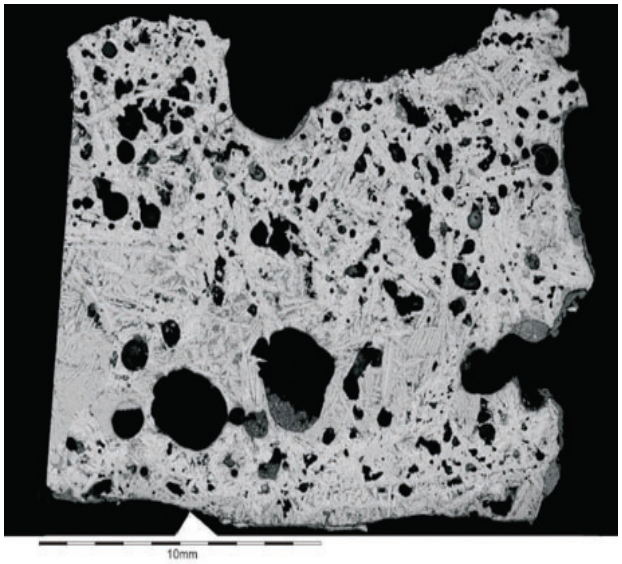

Plate 184: Backscattered electron image - CUT14, whole sample

Smithing slags

Although many of the items with a morphology resembling that of a smithing-hearth cake (SHC) have been demonstrated to have been formed within the base of smelting furnaces (*p 307*), two of the specimens examined can be related to secondary processes with a high degree of confidence.

Sample CUT15: Pit *719* (fill *718*)

This specimen was a 280 g fragment from the rounded margin of a slag cake, with a flat top with broad dimples and somewhat wispy peaks between, and a base with fine dimples and prills, probably into a fuel bed. The margin curves inwards abruptly so the base and top become parallel, 45-50 mm apart. The specimen is very dense, but with abundant large, irregular, internal vesicles. Chemical analysis of this piece shows it to have an exceptionally high iron content.

Sample CUT16: Topsoil (*500*)

This specimen was an approximately plano-convex block, comprising iron set within an extremely

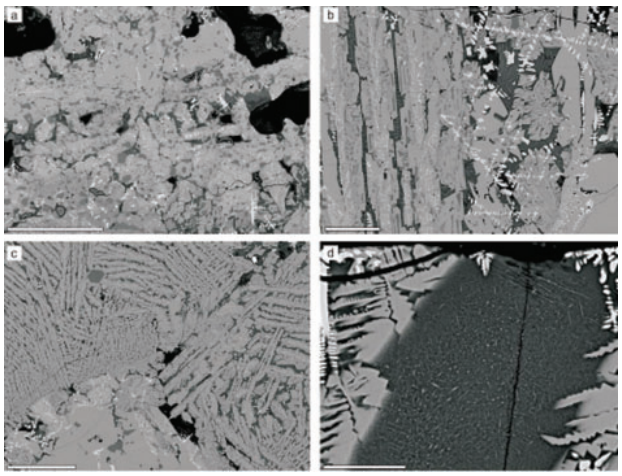

Plate 185: Backscattered electron images - CUT14

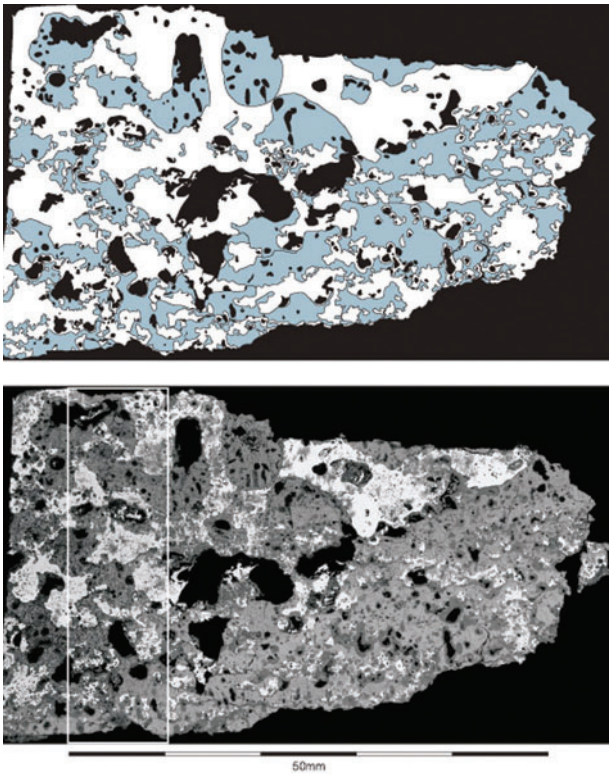

Plate 186: Backscattered electron image of the polished block, covering part of CUT16, and simplified sketch of the polished block

wustite-rich slag. The block as recovered was approximately 160 x 150 x 90 mm thick, with a very slightly dished top and slightly dimpled base, weighing 3765 g.

The section examined (Pl 186) shows a maximum thickness of 40 mm. There is a broad division into two across an oblique divide, marked in part by cavities (Pl 187a). On the cut face of the block (Pl 188), this division can be seen as a layered structure, with the typical size of iron particles increasing upwards. Within the polished mount, two such zones are visible: the upper corresponding to more continuous iron, with large (up to approximately 8 mm) rounded, slag-filled cavities, that are locally interconnected; the lower corresponds to a texture in which the slag is dominant, bearing highly irregular iron particles. In both zones, but particularly the lower, there are small areas in which the metallic iron extends as blebs into the wustitic slag (Pl 187b).

The wustite-rich slag varies in composition across the block. In much of the lower part, the wustite forms more than 95% of the slag, although there are occasional tiny areas in which fayalite is clearly visible. In the upper part, the wustite proportion is typically slightly lower, with the fayalite component clearly visible in the slag

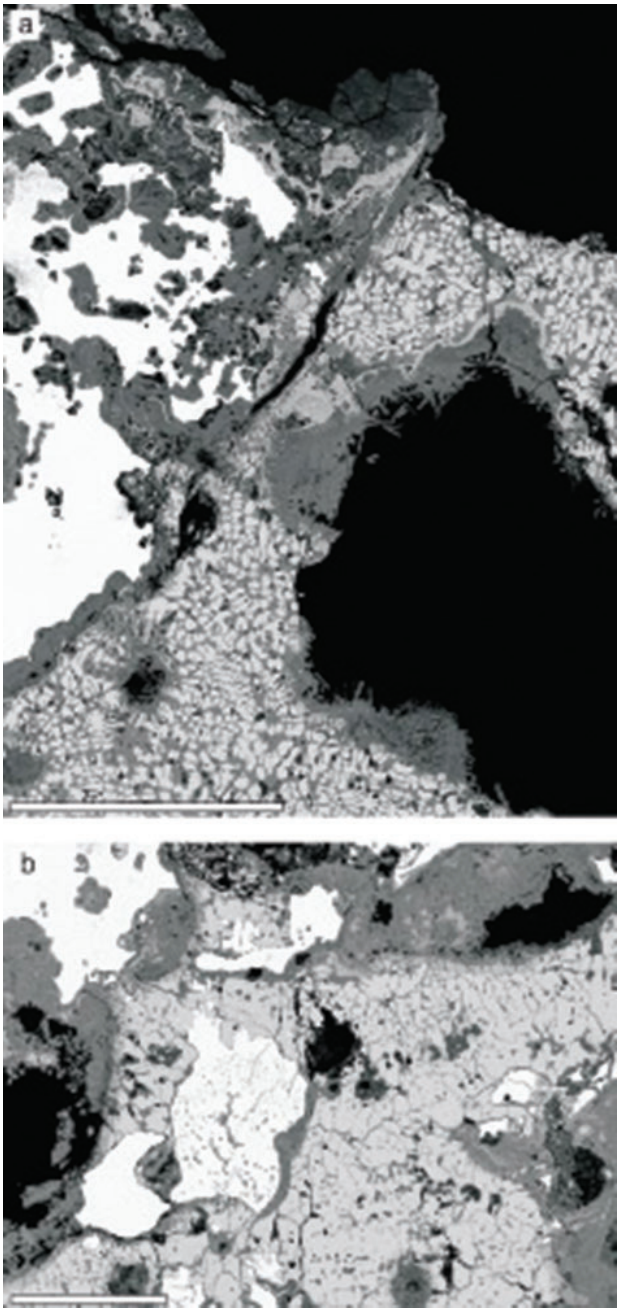

Plate 187: Backscattered electron images – CUT16

filling the large cavities within the metallic iron. The elemental map for manganese (Pl 189) picks out small areas of fayalitic slag within the upper part of the iron; these are likely to be remnant inclusions of smelting slag.

The wustite-rich slag bears small cavities, which may variously be either voids formed by the dissolution of small iron particles or original vesicles, probably mostly the latter. These show an infill of elongate secondary iron oxides. Alteration of the sample is also picked-out by the distribution of chlorine along cracks and the margins of voids.

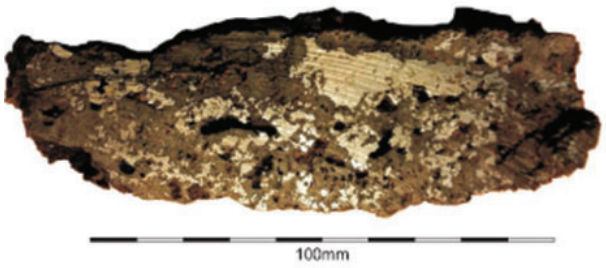

Plate 188: Cut surface through block sampled as CUT16

Lining and lining slag

This material was not common on the site, being a feature typical of redeposited or reworked assemblages. Significant quantities did occur in furnaces ***578*** (*Ch 3, p 48*), ***588*** (*Ch 3, p 44*), and ***722*** (*Ch 3, p 48*), and scoop ***596*** (*Ch 3, p 49*). This material does not contribute to an understanding of the morphology of the furnaces or hearths, however, but it may aid the construction of furnace mass balance (*p 330*).

Ore

The site yielded a low level of finds of claystone ironstone nodules and it is hard to exclude a natural origin for these materials. More significant, perhaps, is the occurrence in pit fill ***597*** (scoop ***596***; *Ch 3, p 49*) of magnetic claystone ironstone, with ores in various stages of slagging.

Iron

Various fragments of iron were identified. These were mostly too badly corroded to be able to be interpreted. One irregular fragment from pit fill ***597*** (*Ch 3, p 49*) showed a strong internal fibrous structure within the corrosion layer, suggesting it was bar iron, rather than a bloom fragment.

Chemical Composition of Residues

The smelting slags formed a homogeneous group (Fig 130). They are moderately aluminous (with a silica:alumina ratio of approximately 4.4 by weight), moderately to strongly manganiferous (typically equivalent to around 1.9-7.1 wt% manganese oxide (MnO)), but have low concentrations of alkalis, magnesium, and calcium (Table 17; Fig 131). Two samples of smelting slags (CUT3 and CUT7) have markedly higher contents of manganese, magnesium, and calcium than do the others; this is likely to reflect a variant on the ore with a higher ankeritic component.

The dominance of the elements iron, manganese, aluminium, and silicon means that the relationship between the samples may be displayed on the FeO-SiO_2-Al_2O_3 ternary diagram (Fig 130; after Schairer

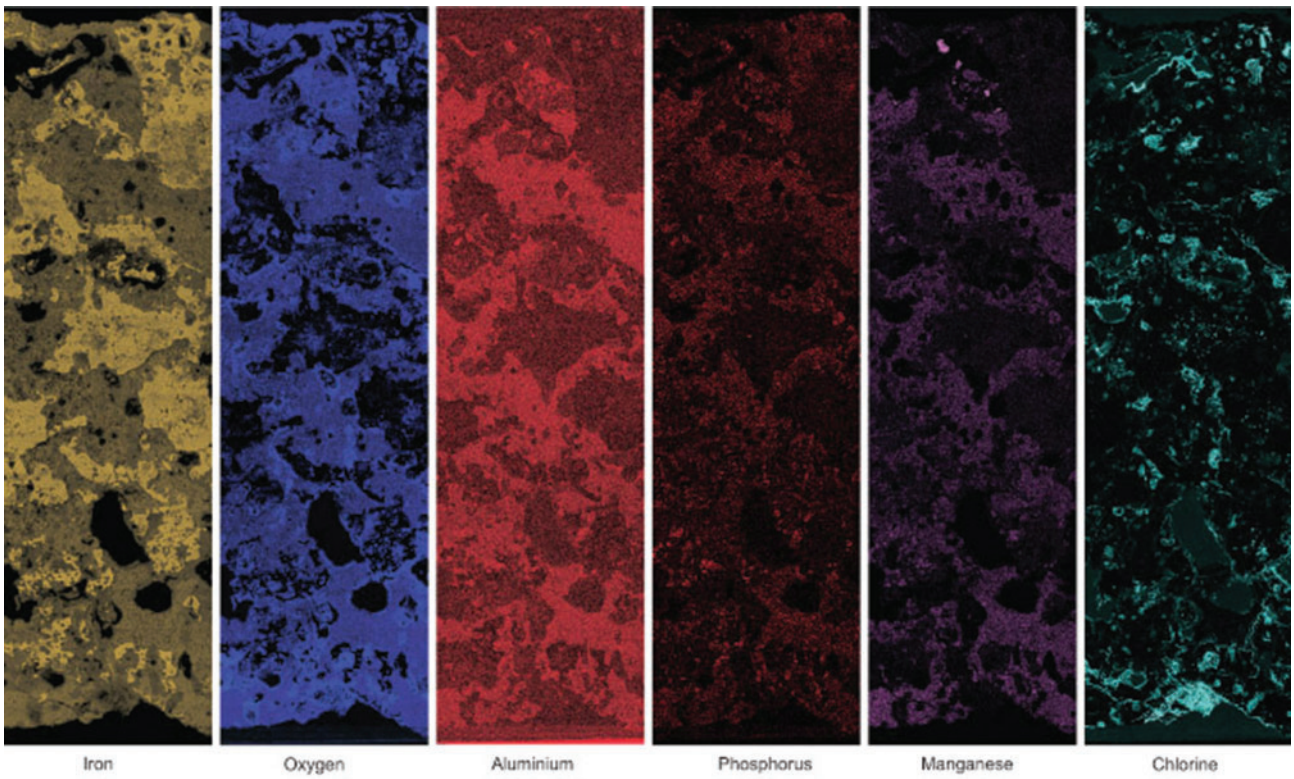

Plate 189: Element mapping of sample CUT16

and Yagi 1952). For the bulk sample compositions (Fig 130a), the majority the smelting slags plot within the fayalite field, with two abnormal, more siliceous, smelting slags plotting outside. When the analyses of sub-areas of the specimens examined by SEM are plotted on the same diagram (Fig 130b), the data from each specimen are tightly clustered. The trace element content of the slags is generally unremarkable and comparable to that of other Coal Measures-sourced assemblages. Some samples are rich in barium (up to 0.75 wt%).

For most samples, the rare earth elements (REE) show an upper-crust normalised profile, with a low, asymmetric, 'hump' in the middle REE (Fig 132). This profile is seen in all the slags (both those attributed to smelting and that believed to be from smithing) and in one of the iron ores (CUT2). The other iron sample (CUT1) shows elevated levels of REE, with a relatively depleted light REEs (Fig 132c). The single sample of furnace ceramic (CUT12) shows a horizontal profile, as would be expected.

The profiles of tapped smelting-slag samples CUT5, CUT7, CUT10, and CUT11 are very tightly clustered (Fig 132b), with only CUT3 and CUT4 having profiles that are elevated above the group. The profiles of all four samples of the biconvex cakes interpreted as being from the furnace base (CUT8, CUT9, CUT13, and CUT14) are similarly tightly clustered (Fig 132a).

The relationship between the REE profiles of the various groups of residues has been plotted (Fig 133). The clustering of the samples from the furnace-slag bowls is very tight, with no overlap with the more enriched samples from the tapped slags. There is overlap between the cluster and the example of ore with a similar profile (CUT2), but with only a single sample of matching ore, the relationship is of uncertain significance.

The examination of the binary relationships between the major elements in the bulk samples (each element is plotted in Figure 131 against silicon as atom%) shows rather variable patterns, with some elements (particularly magnesium, calcium, and manganese) showing a wide range of values within the tapped slags. These elements are those which also occur in siderite as substitutions, or even as other carbonate minerals.

The degree of internal variation within some of the samples is illustrated by the binary plots of various major elements plotted against silicon (as atom %; Fig 134), and against calcium and iron (Fig 135). In these figures, the two analysed tapped-slag samples (CUT5 and CUT7) show different compositions (CUT7 is one of the samples with markedly elevated manganese), but there is little variation within the samples. In contrast, samples CUT13 and CUT14 (taken from the same biconvex slag block) show a high degree of internal variation of most elements except iron and manganese. Many of the elements with the

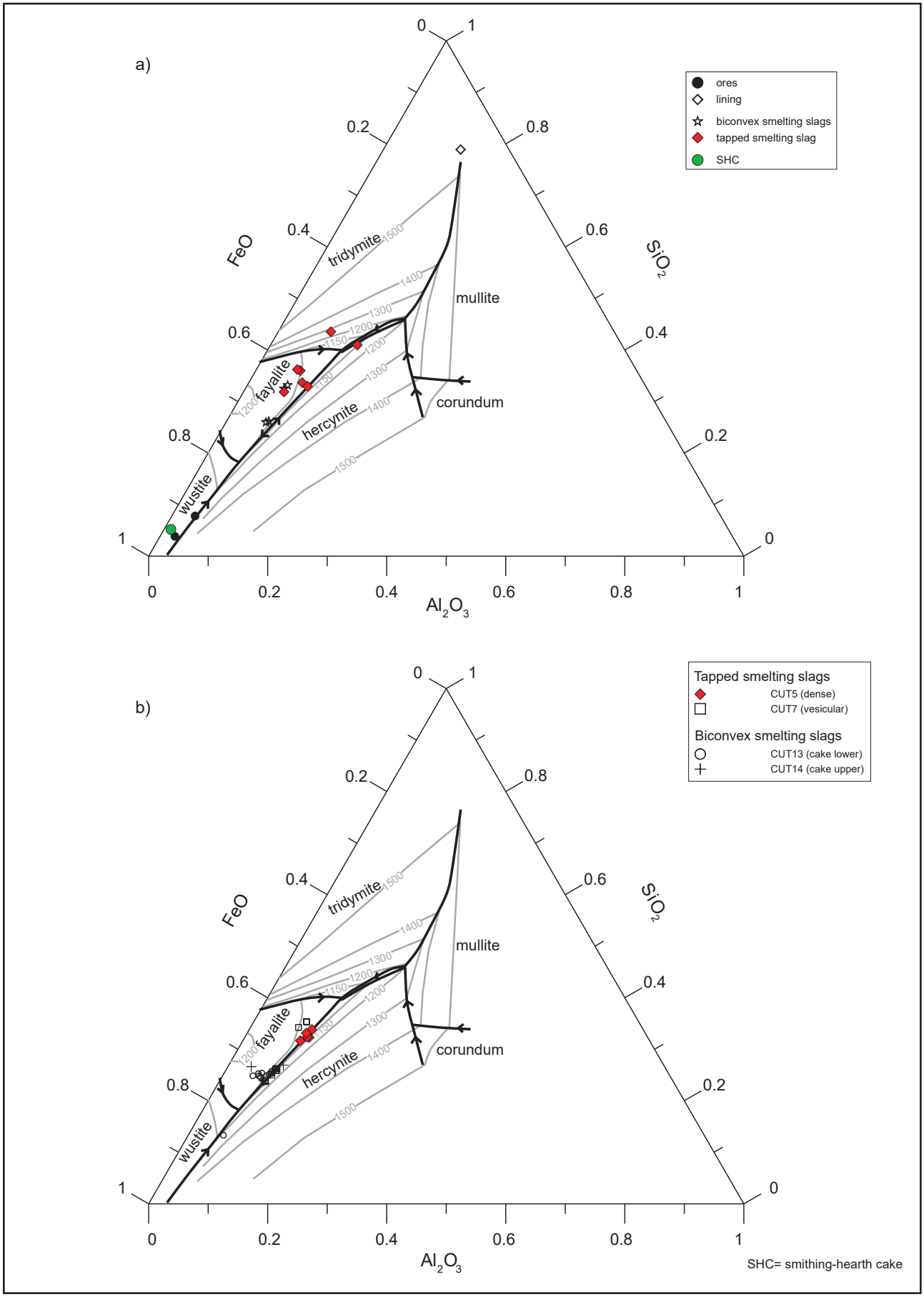

Figure 130: Analyses plotted on FeO–SiO_2–Al_2O_3 ternary diagram

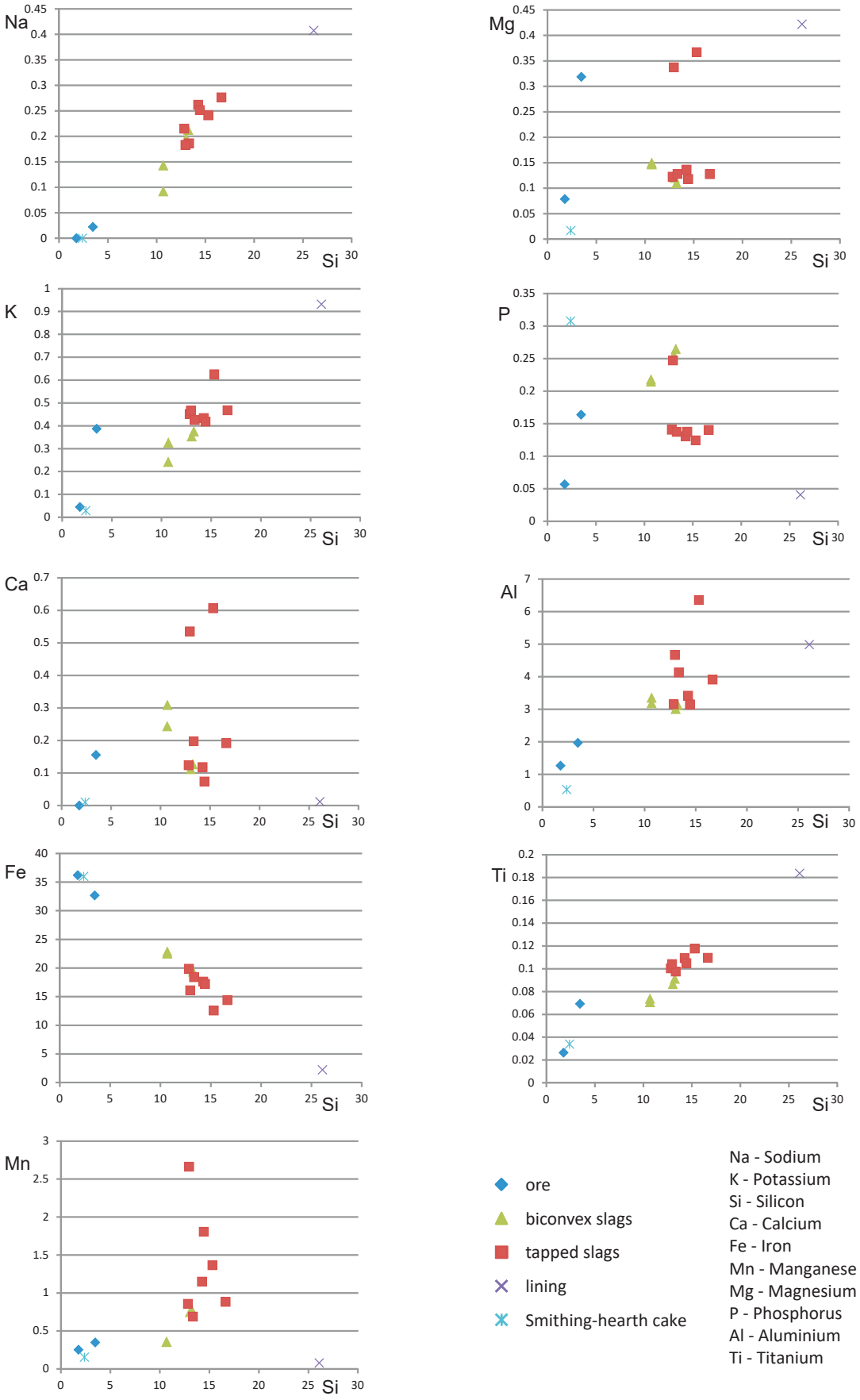

Figure 131: Binary elemental plots (normalised data by ERF) in atom% for bulk slag samples, showing various major elements plotted against atom% silicon

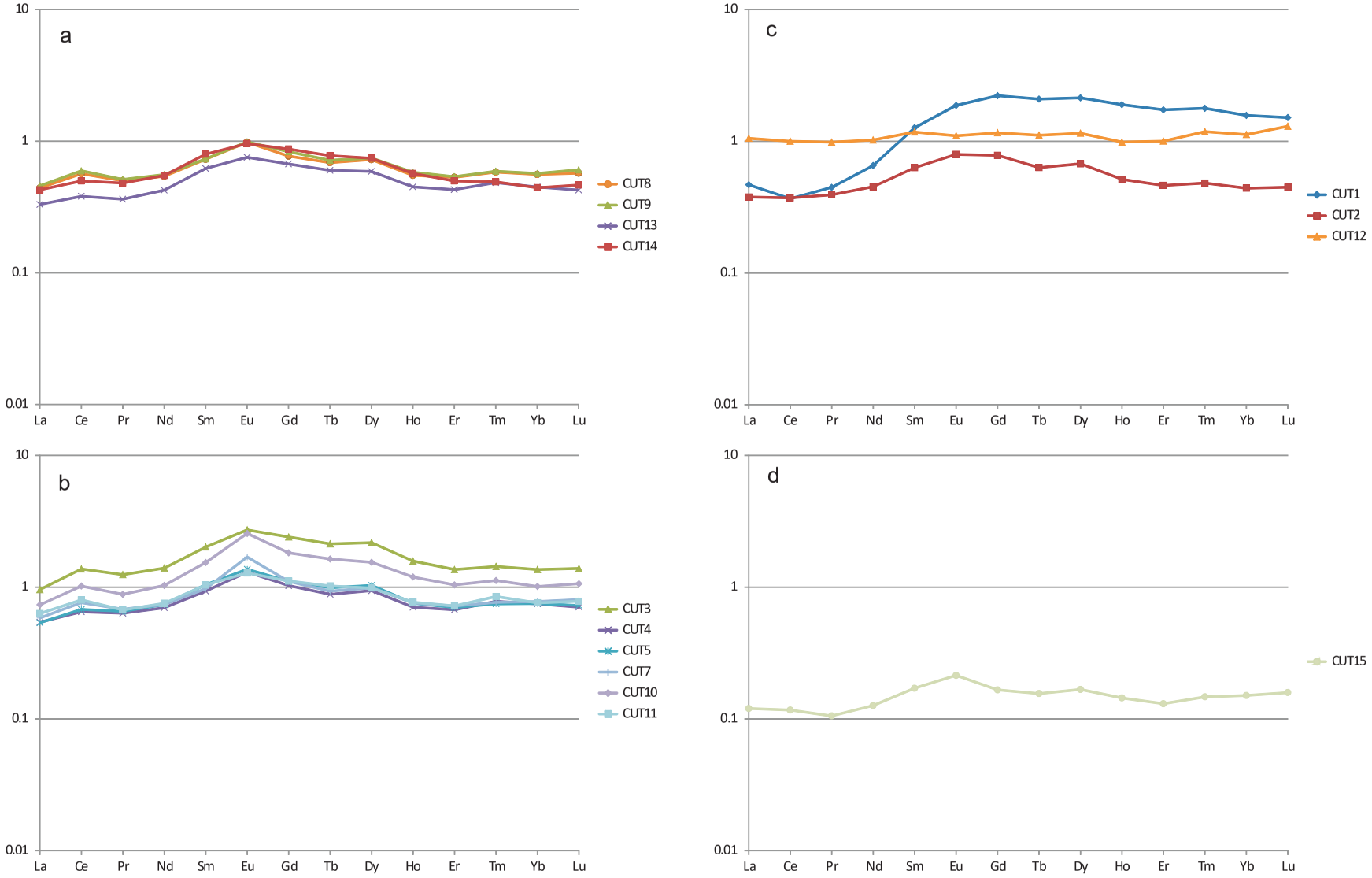

La - Lanthanum, Ce - Cerium, Pr - Praseodymium, Nd - Neodymium, Sm - Samarium, Eu - Europium, Gd - Gadolinium, Tb - Terbium, Dy - Dysprosium, Ho - Holmium, Er - Erbium, Tm - Thulium, Yb - Ytterbium, Lu - Lutetium

Figure 132: Upper crust normalised rare-earth element profiles for furnace ceramics, ore, and slag samples

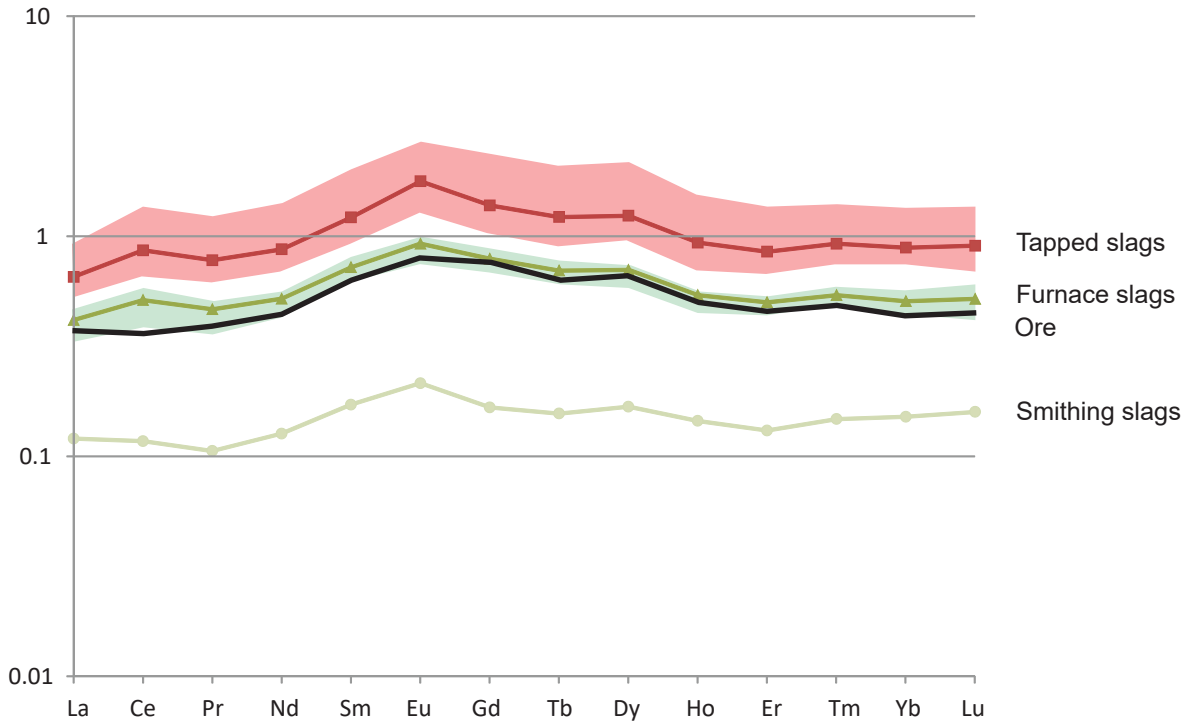

La - Lanthanum, Ce - Cerium, Pr - Praseodymium, Nd - Neodymium, Sm - Samarium, Eu - Europium, Gd - Gadolinium, Tb - Terbium, Dy - Dysprosium, Ho - Holmium, Er - Erbium, Tm - Thulium, Yb - Ytterbium, Lu - Lutetium

Figure 133: Comparison of upper crust normalised rare-earth element profiles

highest degrees of variation within these two samples (*eg* Magnesium (Mg), Calcium (Ca), Potassium (K)) will be present in the fuel ash as well as the ore and furnace materials, giving another possible mechanism for their local variability.

Interpretation

The smelting slags form an approximately coherent suite when plotted on the SiO_2-Al_2O_3-(FeO+MnO) ternary diagram (silica dioxide – aluminium oxide (iron oxide, manganese oxide); Fig 129a), with an average SiO_2:Al_2O_3 ratio of 4.4 by weight. The analyses of the smelting slags mostly plot within the fayalite field, but the two most iron-poor examples (with >37 wt% normalised SiO_2) plot outside. Neither of these two samples (samples CUT3 and CUT11) was typical of the main slag classes from the site. The samples identified morphologically as tapped slags have a range of approximately 57-61% normalised wt% iron; the two cakes interpreted as within-furnace slag-puddles have approximately 61% and 67% normalised wt% iron.

This distribution of analyses within the SiO_2-Al_2O_3-(FeO+MnO) ternary diagram (Fig 129a) is very similar to that recorded for slags from two medieval sites in Shropshire, which had also smelted Coal-Measures iron ores (Young and Poyner 2014, fig 11). The Shropshire slags showed an average SiO_2:Al_2O_3 ratio of 4.4 by weight for those from Ned's Garden, with 2.9 for those from Cinder Mill. The differences were interpreted as reflecting a different host sediment to the claystone ores exploited at the two localities, although slightly different furnace clays may also have influenced the variation.

The variation in the content of calcium, magnesium, and manganese was also a feature noted amongst the Shropshire residues (*op cit*, 90). This can be attributed to the natural variability of the content of siderite concretions, not only between concretions in different seams, but also within individual concretions. Such variability within Coal-Measures ironstones has been discussed within their context as a resource (Young 1993, 466-7) and in detail from a geological perspective (by Curtis and co-workers; Curtis and Spears 1968; Curtis *et al* 1975; 1986a; 1986b).

The large biconvex slag cakes (samples CUT8/9 and CUT13/14) show many morphological and textural features commonly associated with smithing-hearth cakes (SHCs): a biconvex shape; a dense lower section filling the bowl of the cake; a less dense, highly vesicular, upper section; a coarse vertically aligned microstructure, with tubular vesicles in the lower

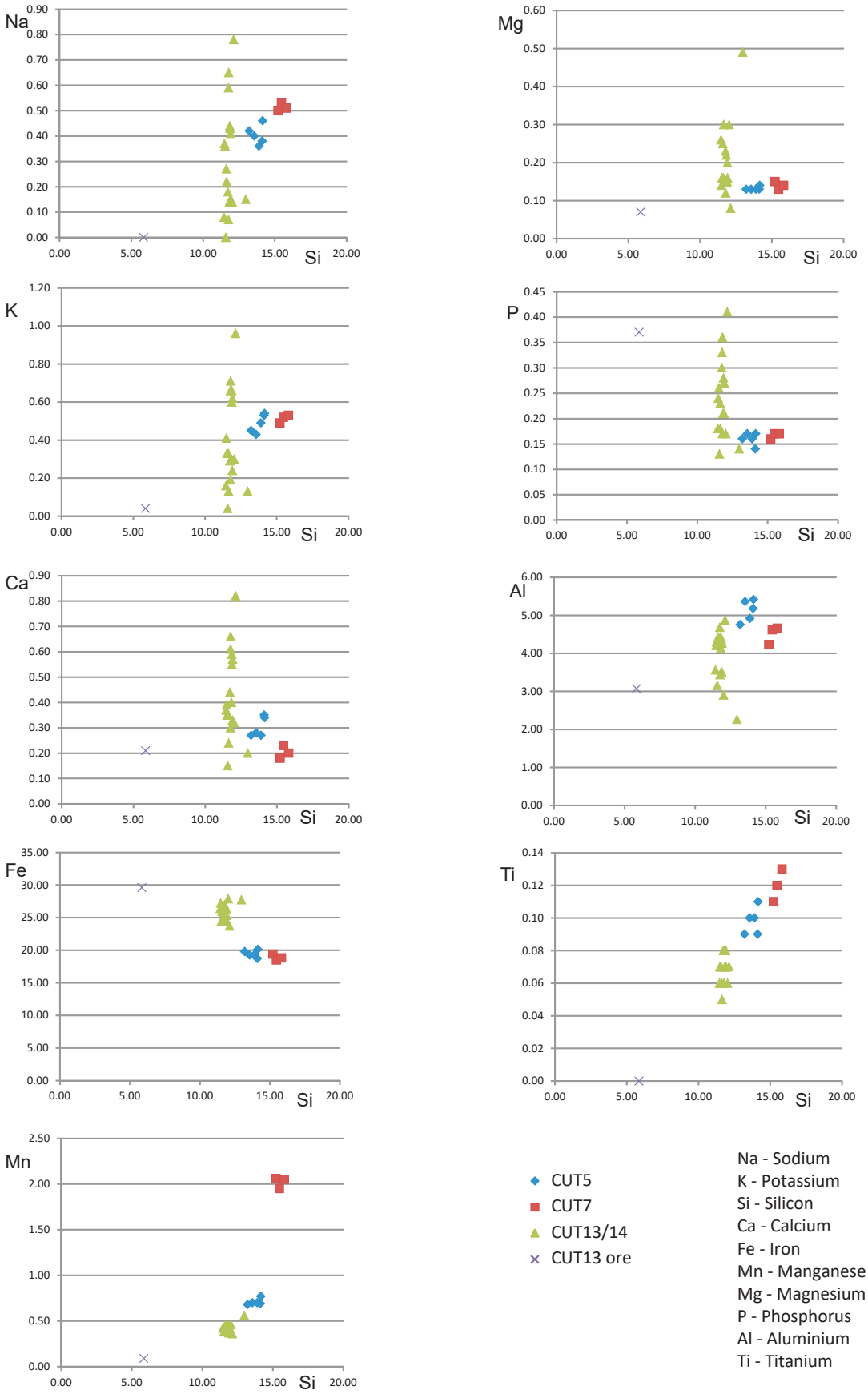

Figure 134: Binary elemental plots (data by EDS) in atom% for sub-areas within slag samples, showing various major elements plotted against atom% silicon

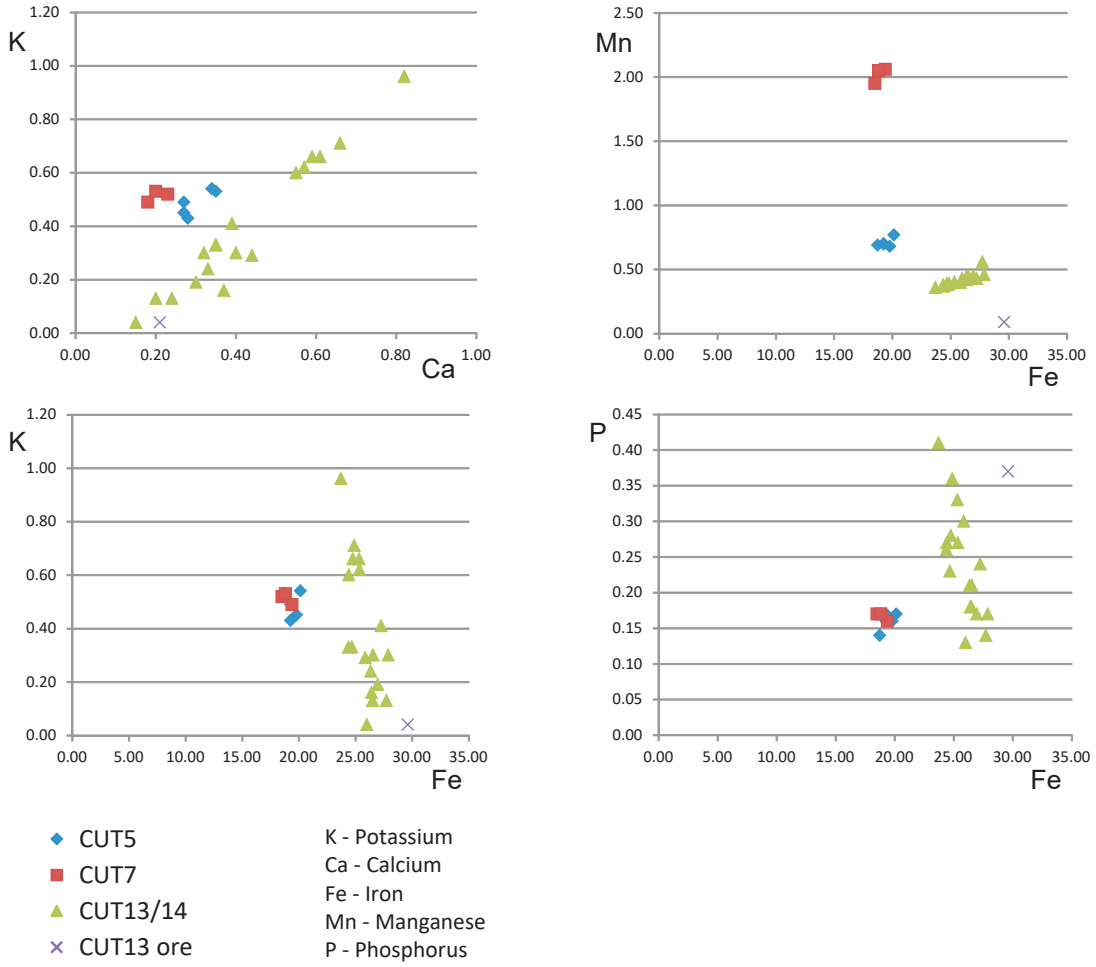

Figure 135: Binary elemental plots (data by EDS) in atom% for sub-areas within slag samples

section; and a smooth to slightly lobate top. Some of the features (such as the hint of a recurved profile to the top, and the separation of sections of the upper section from the lower bowl, with intermediate large rounded cavities) are similar to those observed in slag cakes formed during hearth-remelting processes, in which the slag cake was in close contact with the developing overlying bloom (*pers obs*). A second similar cake (samples CUT8/9) was less complete, but analyses suggested it was very similar to the block providing samples CUT13/14.

The bulk chemical compositions of these cakes, however, closely parallel those of the associated tapped slags and lie on the same trend. The chemical evidence, therefore, strongly suggests that these blocks are smelting slags rather than a smithing slag. This is supported by the presence of an incompletely reacted ore particle within sample CUT13. The variation in composition within the block on a fine scale (both the bulk composition and the degree of variation exhibited by the olivine) is, however, very much greater than that seen within tapped-slag flows. This variation suggests the environment of formation of the slag cake permitted considerable differentiation of the melt. These features, taken together, strongly suggest that these slag cakes were formed progressively inside the smelting furnace and not outside through tapping. It may be significant that the plan of furnace **722**/***720*** (*Ch 3, p 47*) shows the *in-situ* slag flow (**722**) as including a substantial component within the furnace base.

A slag cake of this general form (but weighing approximately 6.3 kg and with a markedly recurved profile to the upper surface) was recovered *in situ* in the base of a furnace (409; twelfth-thirteenth century) at Roughlawn, Wiltshire (*pers obs*; unpublished data), and another similar cake (3.1 kg) was unstratified in an adjacent stream. A smaller (2.5 kg), but very similar, example was also recovered *in situ* in a furnace (131161) at Torr Quarry (Young 2014a; sample TOR1).

Both the *in-situ* cakes from Roughlawn and Torr Quarry were found in place in slag-tapping bloomery furnaces that had received a late relining, above earlier fills in the furnace bowl. This possible modification of the original form of the furnaces gave rise to some doubt as to whether these examples were formed during primary smelting. The Roughlawn

and Torr Quarry examples were all initially interpreted as deriving from secondary process (possibly being from a hearth-remelting process, and the unstratified example from Roughlawn as a smithing-hearth cake from bloomsmithing). Neither of the Roughlawn examples has been analysed. The Torr Quarry example had a composition that matched closely those of the tapped slags from the Cutacre site, as well as the ores (*op cit*, fig 2). There seems little doubt that the Torr Quarry furnaces were capable of producing an internal slag cake, as well as the externally tapped slags.

The Cinder Hill furnaces show some morphological similarity with those of Torr Quarry, in having well-developed furnace bowls, which would be capable of 'ponding' slag, instead of allowing it to flow through the tapping channel. It therefore seems likely that the biconvex slag cakes from Cutacre may be attributed to smelting and not to smithing, as initially envisaged.

Taken together, these slag blocks, not only from Cutacre, but also from Roughlawn and Torr Quarry, suggest a previously unrecognised aspect of twelfth-thirteenth-century iron smelting, namely that the process (at least on occasion) entailed the formation of a 'puddle' of slag within a hollow in the floor of the furnace. The bloomery process, as undertaken by most modern reproductions of slag-tapping furnaces (*cf* Sauder and Williams 2002), involves a slag 'bowl' in which the bloom develops, typically at a high level in the furnace base, sometimes partially supported by a bed of ash or charcoal fines, which leaks slag during tapping. This bowl is not in contact with furnace substrate, unlike most of the medieval examples. Only the *in-situ* example from Roughlawn was suspended above the clay floor on the tapping-arch side of the hearth. Formation of a slag bowl in contact with the base of the furnace may cause problems with the preparation of the furnace for the subsequent smelt, for the slag block would be hard to prise from the substrate. It is possible, therefore, that these dense basal slag cakes were not intended to lie on the base, and that their unintentional formation in that location in these examples was what precipitated abandonment of the furnace.

The recognition of the biconvex slag cakes as a significant component of the smelting-residue assemblage, and their distinct composition compared with the tapped slags, means that their composition must be taken into account when modelling the furnace mass balance. It is not yet certain that the bowls were a normal part of the residue assemblage from regular smelts; it is possible that they formed only in over-deepened furnace bases. This point requires further investigation from large assemblages.

The modelling of the furnace productivity is further complicated by the complete absence in the studied assemblage of intact tapped slag cakes. If the majority of the crust and bowl fragments (Table 15) are smelting residues (biconvex cakes) and not smithing-hearth cakes, then there might be as much as 30 kg of such cakes alongside perhaps 150 kg of tap slag (*ie* a ratio of 1:5 between these slag classes). Individual tapped-slag cakes at Roughlawn (*pers obs*) were up to approximately 11 kg and the site also produced plano-convex cakes weighing 2.5 kg, and perhaps as much as 6 kg (the 6.3 kg sample includes a much-adhering furnace lining), giving ratios of 1:4.4 and 1:1.8 respectively. At Torr Quarry (Young 2014a, 8), individual recorded tapped-slag flows weighed 16 kg (131149), 15 kg (13290), and 14 kg (13295), and the internal slag cake weighed 2.5 kg (a ratio of approximately 1:6). On this basis, it is quite plausible that the ratio of slag types at Cutacre does represent regular production, rather than irregular, accidental production.

The wustite-rich slag cakes are a facies of slag that has not been adequately described in the past. Slags dating to the Iron Age to Roman period interpreted as having been produced during bloom-smithing have been recognised (Site 331 on the Brecon-Tirley pipeline; Young 2012, 3-5; Neath; Young 2014c). In both cases some of the particularly iron-rich material shows oxidation as far as iscorite (iron silicate) and magnetite (iron oxide), a feature not observed in the Cutacre material. It is also noteworthy that these early bloom-smithing slags have zones of much higher silica content. The higher silica content of the early slags may represent a greater consumption of the hearth wall during the compaction process than was the case in the Cutacre material. This might be due to a more prolonged process, or to the use of a hearth geometry or ceramic tuyère, that melted more quickly. The medieval smelting site at Llwyn Du has produced smithing slags rich in fragments of both high carbon and cast iron (P Crew *pers comm*).

Perhaps the most likely interpretation of the larger block (sample CUT16) is that it represents the accumulation, in the hearth, of debris from the compaction of a bloom or blooms. Rapid oxidation of the hot metal has produced abundant wustite, which provides a slag matrix to those pieces of iron that became detached and sank through the hearth sufficiently quickly to avoid oxidation. In the case of the smaller example (sample CUT15), there is no evidence for the survival of metallic iron.

The estimation of production at Cinder Hill is made somewhat problematic by the nature of the ore. Attempts to construct a mass balance for the smelting reaction by employing the technique of Thomas and

Young (1999a; 1999b) with the analyses of the Cinder Hill materials failed to generate a viable, coherent solution. The implication of this is that, although the REE profile of the weathered ore sample, CUT2, indicated this ore had the same REE signature as the exploited resource, its bulk chemical composition was incompatible. The most likely reason for this was that the ore smelted at Cinder Hill would have been roasted sideritic claystone ore, not the highly weathered oxidised remnants surviving in samples CUT1 and CUT2. Without an appropriate ore sample, therefore, the mass balance cannot be calculated.

The scale of production is similarly problematic. If the weight of slag produced in one smelt was of the order of 15 kg (by comparison with the contemporary sites at Torr Quarry and Roughlawn; *p 330*), then the total assemblage of 200 kg represents the equivalent of the residues from just 13 smelts, whereas each of the furnaces would have been capable of being used for certainly many tens and probably several hundreds of smelts. An excavated early medieval iron-smelting site at Culmstock Road, Hemyock, Devon, with a similar number of features to the Cinder Hill site and covering a similar area, but with the early medieval deposits protected by a layer of colluvium, produced an estimated 22 tonnes of slag (*pers obs*). It is thus likely that large amounts of slag have been lost from the Cinder Hill site, either through agricultural activity or through deliberate quarrying of the slag for resmelting in post-medieval blast furnaces. The presence of between two and six furnaces indicates a site of significant and/or repeated use, but the actual scale of production is not able to be determined.

Conclusion

The assemblage of industrial residues from Cinder Hill is small compared with the amount of residues that must have been produced by the multiple furnaces, and most of the slag has probably been dispersed by subsequent agricultural activity. Indeed, the furnace remains themselves were heavily truncated by later agricultural activity. Nonetheless, the surviving evidence places Cinder Hill comfortably within the small corpus of twelfth- to fourteenth-century bloomery sites and residue assemblages. The relatively small amount of surviving residue means it is impossible to determine the level, total, or significance of overall production, although the multiple furnaces indicate that the site may have been used, either continuously or repeatedly, over a considerable period of time, contrasting with the modest surviving residue assemblage.

The site was probably smelting the local Carboniferous claystone ironstones from the Coal Measures. There was no evidence for the iron ore actually cropping out on the site, and thus other factors may have influenced the location of the smelting activity at this particular location. A movement of bloomery furnaces through coppiced woodland with the coppice rotation has been documented elsewhere (*cf* Smith 1995; Crew and Crew 2001) and this might have been the case at Cinder Hill, giving rise to multiple furnaces (with a new furnace perhaps being constructed on each return to the location with the coppicing cycle), perhaps with quite modest use. Such use was probably what was implied by the term *forgiaeerrantes* in descriptions of bloomery-iron smelting in the Forest of Dean during the medieval period (Nicholls 1866). However, that said, no evidence for coppicing was present in the charcoal assemblage recovered from the charcoal clamp at the site (*Appendix 5*).

The evidence for the processing of blooms is very limited. Wustite- and/or metallic iron-rich cakes were identified, which may indicate the initial stage of compaction of the fresh blooms. Although there was no evidence for the more conventional smithing-hearth cakes that would have been produced if the iron had been fully worked down to bar or billet on site, one possible fragment of bar iron was recovered.